

# Structured Linearization of Discrete Mechanical Systems for Analysis and Optimal Control

Elliot Johnson, Jarvis Schultz, and Todd Murphey

**Abstract**—Variational integrators are well-suited for simulation of mechanical systems because they preserve mechanical quantities about a system such as momentum, or its change if external forcing is involved, and holonomic constraints. While they are not energy-preserving they do exhibit long-time stable energy behavior. However, variational integrators often simulate mechanical system dynamics by solving an implicit difference equation at each time step, one that is moreover expressed purely in terms of configurations at different time steps. This paper formulates the first- and second-order linearizations of a variational integrator in a manner that is amenable to control analysis and synthesis, creating a bridge between existing analysis and optimal control tools for discrete dynamic systems and variational integrators for mechanical systems in generalized coordinates with forcing and holonomic constraints. The forced pendulum is used to illustrate the technique. A second example solves the discrete LQR problem to find a locally stabilizing controller for a 40 DOF system with 6 constraints.

**Note to Practitioners**—The practical value of this work is the explicit derivation of recursive formulas for exact expressions for the first- and second-order linearizations of an arbitrary constrained mechanical system without requiring symbolic calculations. This is most applicable to the design of computer-aided design (CAD) software, where providing linearization information and sensitivity analysis facilitates mechanism analysis (e.g., controllability, observability) as well as control design (e.g., design of locally stabilizing feedback laws).

**Index Terms**—simulation, mechanism analysis, optimal control

## I. INTRODUCTION

NUMERICAL integration schemes for mechanical systems typically begin with continuous-time representations of dynamics (i.e., ordinary differential equations) and then apply numerical integration to yield a discrete-time approximation to the continuous-time dynamics. Instead of computing the Euler-Lagrange equations based on extremizing the action integral, variational integrators—sometimes referred to as *structured integrators* [1]—use a time-discretized form of the action integral and then the resulting action sum is extremized. The subsequent integrators have the advantage of conserving momentum and a symplectic form as well as bounding energy behavior [2]. Hence, variational integrators avoid the calculation of any ordinary differential equations (ODE) and lead to an implicit difference equation that is solved numerically at each time step to find the next configuration of

a mechanical system. Additionally the numeric properties of variational integrators typically provide stable energy behavior over long time horizons even with large timesteps [3] while also providing exact holonomic constraint satisfaction [4].

Despite the fact that variational integrators simulate a system by numerically solving an implicit non-linear equation at each time step, the process can be abstractly represented in state form as an explicit, one-step discrete dynamic system (i.e.,  $x_{k+1} = f(x_k, u_k)$ ) [1]. The contribution of this work is to calculate the first- and second-order linearizations of this abstracted form, and it is useful that the linearization may be explicitly calculated without ever calculating an analytic expression for the one-step map itself. This approach makes variational integrators compatible with a wide range of existing analysis and optimal control tools for discrete dynamic systems (e.g., LQ regulators [5], predictive control in assembly [6], deconvolution techniques [7]). The methods described apply to complex mechanical systems in generalized coordinates with many degrees of freedom and holonomic constraints, such as those previously studied in [8].

The importance of linear systems analysis is evident in nearly all engineering analysis, but computing linearizations can be analytically challenging (e.g., computing transverse linearizations for periodic systems [9]) and moreover computing the discrete time linearization from the continuous one is susceptible to substantial numerical difficulties [10]. By taking advantage of discrete-time variational integrators we obtain exact representations of the discrete-time linearization for arbitrary mechanical systems subject to holonomic constraints.

Existing literature discusses linearizing variational integrators [11] for the purpose of constructing more accurate integrators. That approach linearizes the discrete Lagrangian itself before the action principle is applied. The method described in this paper is specifically for analysis and optimal control applications that require linearizations of the dynamics, after the action principle is invoked.

Without the state form representation and linearizations discussed in this paper, the implicit form of a variational integrator is incompatible with the majority of existing analysis and optimal control techniques for discrete systems described by an explicit first-order state form [5]. Applications that require more than simulation (e.g. stability analysis, design of feedback control laws, optimal control) force the designer to either build an auxiliary model with traditional continuous dynamics—that are only guaranteed to apply to the discrete-time model in the limit as  $dt \rightarrow 0$ —or develop new methods specific to variational integrators.

The Discrete Mechanics Optimal Control (DMOC) frame-

Elliot Johnson is with the Southwest Research Institute, San Antonio, TX, 78228 USA (e-mail: elliot.johnson@swri.org). His work was performed while a graduate student at Northwestern University.

Jarvis Schultz, and Todd Murphey are with the Department of Mechanical Engineering, Northwestern University, Evanston, IL, 60201 USA. (e-mail: jschultz@u.northwestern.edu, t-murphey@northwestern.edu)

work [12], [13] offers such an approach to optimal control based on variational integrators. DMOC was developed to replace infinite dimensional, continuous time optimal control problems with an (approximately) equivalent finite-dimensional, constrained optimal control problem. The optimal control problem can then be solved using standard numeric optimization methods without the problems associated with numeric integration and infinite dimensional vector spaces. One of the contributions of this paper is that we supplement DMOC by connecting variational integrators with existing discrete optimal control methods, providing the capability to take an optimal trajectory generated by DMOC and generate a feedback regulator for it. In [14] DMOC is used to generate a discrete reference trajectory for the swing-up of a cart-pendulum system. In order to generate stabilizing feedback controllers about this trajectory, the authors utilize interpolation to provide a continuous representation of the discrete trajectory and thus allow standard linearizations. A gain-scheduling technique is then used to piece together solutions to a set of continuous LQR controllers, which are then presumably implemented experimentally in discrete time. The discrete linearizations presented herein allow this entire process to occur in discrete time. Similarly, the techniques discussed here could be used to generate feedback laws for planning algorithms that provide plans in configuration space [15].

In [12], it is shown that the discrete-time adjoint equation—the equation that governs optimality of a control signal—for an explicit/implicit partitioned Runge-Kutta scheme is itself an explicit/implicit partitioned Runge-Kutta scheme. Given that result, it is perhaps surprising that the linearization of the (typically) implicitly defined variational integrator is in fact an explicit calculation if the “state” of the system is chosen appropriately. It is by no means obvious that an implicit equation expressed directly in terms of the configuration even has a linearization to which classical methods in discrete-time optimal control can be applied. The key observation is that because a variational integrator can be rewritten as a one-step method (due to the existence of a so-called generating function that generates the method and guarantees its symplecticity), the one-step method provides the appropriate object to linearize. Moreover, another consequence of the existence of the generating function is the existence of a modified Hamiltonian for the system—a system of which the variational integrator is exactly sampling at time steps  $dt$ . This provides another interpretation of the linearization we calculate here—it is both the *exact* discrete-time linearization of the variational integrator as well as the *exact* continuous-time state transition matrix for the modified system evaluated at times that are  $dt$  apart. This correspondence between the discrete-time interpretation and the continuous-time interpretation indicates that the linearization of the map is structure-preserving as well (e.g., the linearization does not artificially introduce non-mechanical behavior by virtue of sampling the trajectory).

The contribution of this paper is thus two-fold. First, we show that the linearization of a variational integrator—in this case that obtained by using the midpoint rule—is explicit despite the variational integrator being implicitly defined.

Moreover, calculating the linearization is simply a matter of following a tree structure that describes the mechanical system, even for constrained systems. We show the second derivative of a trajectory may be obtained as well. The consequence of this result is that linearization information may be obtained in a purely algorithmic foundation, without any symbolic computation; hence, it is reasonable to expect computer aided design (CAD) software packages to include linearization capability for arbitrary topologies for any given numerical method to facilitate analysis and control design for complex mechanisms, potentially operating in scenarios where managing sensitivity is crucial (see, for example, the editorial on this topic [16] where software support of design is cited as a major need in automation). Secondly, we demonstrate that the control calculation is well-posed even for high degree-of-freedom systems, using a stabilization problem for a mechanical model of a 40 DOF marionette as an example. We additionally briefly describe the software package, `trep`, that we have written that implements these techniques as well as corresponding techniques for continuous-time dynamics (the continuous-time dynamics are discussed in [17]).

This paper is organized as follows. Section II describes the particular variational integrator used through the paper, and introduces a pendulum example that is used to demonstrate the methods as they are derived. Section III introduces the abstract representation of a variational integrator as a first-order discrete dynamic system. After the background in Secs. II and III, the first- and second-order linearizations are derived in Sec. IV and V, respectively. The linearizations are extended to include systems with holonomic constraints in Sec. VI. Section VII presents several examples illustrating singularities of the linearizations. An open source software implementation called `trep` is introduced in Sec. VIII and used to find stabilizing feedback controllers first for the simple pendulum in Sec. VIII-A and then for a humanoid marionette in Sec. VIII-B (this example serves as our canonical example of a “complex” underactuated mechanism [18]). Finally, Sec. IX summarizes the method, discusses the advantages and limitations, and discusses future work.

## II. VARIATIONAL INTEGRATORS

In this section we provide a brief overview of variational integrators and present the specific variational integrator used throughout this paper. More detailed introductions and discussions can be found in [4], [19]–[21].

The idea behind variational integrators is to discretize the action with respect to time before finding the discrete-time equations of motion. Doing so leads to integration schemes that avoid problems associated with numerically integrating a continuous ODE. These problems can occur because the numerical approximations that are introduced do not respect fundamental mechanical properties like conservation of momentum, energy, and a symplectic form, all of which are relevant to mechanical systems (both forced and unforced).

The continuous-time dynamics of a mechanical system are described by the Euler-Lagrange equation [22]

$$\frac{d}{dt} \frac{\partial L}{\partial \dot{q}} - \frac{\partial L}{\partial q} = F(q, \dot{q}, u)$$

where  $q$  is the system's generalized coordinates,  $u$  represents the external inputs (e.g, motor torque),  $L$  is the Lagrangian (typically kinetic energy minus potential energy for finite-dimensional mechanical systems), and  $F$  is the forcing function that expresses external forces in the generalized coordinates.

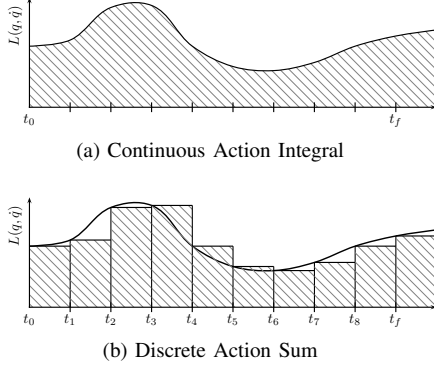


Fig. 1. The continuous Euler-Lagrange equation is derived by minimizing the action integral (a). The discrete Euler-Lagrange equation is derived by minimizing the approximating action sum (b).

The Euler-Lagrange equations can be derived from extremizing the action integral, typically referred to as the (least) action principle. The action integral—the integral of the Lagrangian with respect to time along an arbitrary curve in the tangent bundle—is illustrated as the shaded region in Fig. 1a. The action principle stipulates that a mechanical system will follow the trajectory that extremizes the action with respect to variations in  $q(t)$ . Applying calculus of variations to the action integral shows that it is extremized by the Euler-Lagrange equation.

A variational integrator is derived by choosing a discrete Lagrangian,  $L_d$  that approximates the action over a discrete time step:

$$L_d(q_k, q_{k+1}) \approx \int_{t_k}^{t_{k+1}} L(q(s), \dot{q}(s)) ds$$

where  $q_k$  is a discrete-time configuration that approximates the trajectory (i.e,  $q_k \approx q(t_k)$ ). This approximation can be achieved with any quadrature rule; more accurate approximations lead to more accurate integrators [21]. A concrete example of a discrete Lagrangian approximation is in Sec. II-A.

By summing the discrete Lagrangian over an arbitrary trajectory, the action integral is approximated by a discrete action, as shown in Fig. 1. The action principle is then applied to the action sum to find the *discrete trajectory* that extremizes the discrete action. The result of this calculation is the discrete Euler-Lagrange (DEL) equations:

$$D_2 L_d(q_{k-1}, q_k) + D_1 L_d(q_k, q_{k+1}) = 0$$

where  $D_n L_d$  is the *slot derivative*<sup>1</sup> of  $L_d$ .

The DEL equation depends on the previous, current, and future configuration (but it does not depend on the velocity,

<sup>1</sup>The slot derivative  $D_n L(A_1, A_2, \dots)$  represents the derivative of the function  $L$  with respect to the  $n$ -th argument,  $A_n$ . In many cases, the arguments to the function  $L$  will be dropped for clarity and compactness. Hence, it is helpful to keep in mind that the slot derivative applies to the argument order provided in a function's definition.

making this integrator an appealing representation of dynamics for embedded systems that measure configurations but not velocities). The DEL equation can also be written in an equivalent *position-momentum* form that only depends on the current and future time steps:

$$p_k + D_1 L_d(q_k, q_{k+1}) = 0 \quad (1a)$$

$$p_{k+1} = D_2 L_d(q_k, q_{k+1}) \quad (1b)$$

where  $p_k$  is the discrete momentum of the system at time  $k$ . (By these definitions, it should be clear that  $-D_1 L_d(q_k, q_{k+1})$  and  $D_2 L_d(q_k, q_{k+1})$  are both playing the role of a Legendre transform in discrete time, and are accordingly referred to as the left and right Legendre transforms.)

Equation (1) imposes a constraint on the current and future positions and momenta. Given an initial state  $p_k$  and  $q_k$ , the implicit equation (1a) is solved numerically to find the next configuration  $q_{k+1}$ . In general, (1a) is a non-linear equation that cannot be solved explicitly for  $q_{k+1}$ . In practice, the equation is solved using a numeric method such as the Newton-Raphson algorithm. The next momentum is then calculated explicitly by (1b). After an update,  $k$  is incremented and the process is repeated to simulate the system for as many time steps as desired.

Variational integrators can be extended to include non-conservative forcing (e.g., a motor torque or damping) by using a discrete form of the Lagrange-d'Alembert principle [12]. The continuous force is approximated by a left and right discrete force,  $F_d^-$  and  $F_d^+$ :

$$\begin{aligned} \int_{t_k}^{t_{k+1}} F(q(s), \dot{q}(s), u(s)) \cdot \delta q ds \\ \approx F_d^-(q_k, q_{k+1}, u_k) \cdot \delta q_k + F_d^+(q_k, q_{k+1}, u_k) \cdot \delta q_{k+1} \end{aligned}$$

where  $u_k$  is the discretization of the continuous force inputs:  $u_k \approx u(t_k)$ . As with the discrete Lagrangian, the discrete forcing can be approximated by any quadrature rule. Certain quadrature rules may result in  $F_d^\pm$  also being a function of  $u_{k+1}$  e.g. see [12]. As we want to eventually apply classic control analysis and synthesis techniques, we restrict our choice of quadrature rules to those where  $F_d^\pm$  is independent of  $u_{k+1}$ , largely to keep the resulting linearization of the dynamics causal with respect to the input  $u$ . A concrete example is presented in Sec. II-A.

For clarity, we use the following abbreviations for the discrete Lagrangian and discrete forces throughout this paper:

$$\begin{aligned} L_k &= L_d(q_{k-1}, q_k) \\ F_k^\pm &= F_d^\pm(q_{k-1}, q_k, u_{k-1}). \end{aligned}$$

The forced DEL equations are then:

$$p_k + D_1 L_{k+1} + F_{k+1}^- = 0 \quad (2a)$$

$$p_{k+1} = D_2 L_{k+1} + F_{k+1}^+. \quad (2b)$$

Again, (2) provides a way to calculate the configuration and momentum at the next time step from the current time step. Given the previous state ( $p_k$  and  $q_k$ ) and the current input ( $u_k$ ), the next configuration is found by implicitly solving (2a). The momentum at the next time step is then calculated explicitly by (2b).

In the following section, we provide an example of a variational integrator for a simple one dimensional system. We will use this example to help keep the calculations as concrete as possible during the development of the structured linearization results.

### A. Example: Pendulum

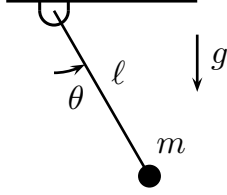


Fig. 2. The pendulum is controlled by a torque at the pivot and subjected to the force of gravity  $g$ .

Consider the pendulum shown in Fig. 2 with  $m = \ell = 1$  and a gravitational force  $g = 9.8$ . All units are assumed to be base units in SI. The pendulum has a single degree of freedom  $\theta$ , is controlled by a torque  $u$  applied at the base, and is subjected to the acceleration due to gravity  $g$ . The Lagrangian for the pendulum is

$$L(\theta, \dot{\theta}) = \frac{1}{2}m\ell^2\dot{\theta}^2 + mg\ell \cos \theta = \frac{1}{2}\dot{\theta}^2 + g \cos \theta.$$

The generalized force due to the torque input is:

$$F(\theta, \dot{\theta}, u) = u.$$

The discrete Lagrangian is found by approximating the integral of the continuous-time Lagrangian over a short time interval  $\Delta t$  using the midpoint rule  $\theta = \frac{\theta_k + \theta_{k+1}}{2}$  and  $\dot{\theta} = \frac{\theta_{k+1} - \theta_k}{\Delta t}$ .

$$L_d(\theta_k, \theta_{k+1}) = L\left(\frac{\theta_k + \theta_{k+1}}{2}, \frac{\theta_{k+1} - \theta_k}{\Delta t}\right) \Delta t \quad (3a)$$

$$= \frac{(\theta_{k+1} - \theta_k)^2}{2\Delta t} + g\Delta t \cos \frac{\theta_{k+1} + \theta_k}{2}. \quad (3b)$$

The forcing is approximated with a combination of a midpoint and forward rectangle rule (though other choices of quadrature would be fine as well):

$$F_d^-(\theta_k, \theta_{k+1}, u_k) = F\left(\frac{\theta_k + \theta_{k+1}}{2}, \frac{\theta_{k+1} - \theta_k}{\Delta t}, u_k\right)\Delta t = u_k \Delta t$$

$$F_d^+(\theta_k, \theta_{k+1}, u_k) = 0.$$

The first derivatives of  $L_d$  are needed to implement the variational integrator in (2):

$$D_1 L_{k+1} = -\frac{\theta_{k+1} - \theta_k}{\Delta t} - \frac{g\Delta t}{2} \sin \frac{\theta_{k+1} + \theta_k}{2} \quad (4)$$

$$D_2 L_{k+1} = \frac{\theta_{k+1} - \theta_k}{\Delta t} - \frac{g\Delta t}{2} \sin \frac{\theta_{k+1} + \theta_k}{2}. \quad (5)$$

The variational integrator update equations are found by substituting (4) into (2a) and (5) into (2b):

$$p_k - \frac{\theta_{k+1} - \theta_k}{\Delta t} - \frac{g\Delta t}{2} \sin \frac{\theta_{k+1} + \theta_k}{2} + u_k \Delta t = 0 \quad (6a)$$

$$p_{k+1} = \frac{\theta_{k+1} - \theta_k}{\Delta t} - \frac{g\Delta t}{2} \sin \frac{\theta_{k+1} + \theta_k}{2}. \quad (6b)$$

Choose initial conditions  $p_k = 0.5$ ,  $q_k = \theta_k = 0.2$ , a time step of  $\Delta t = 0.1s$ , and an applied torque

$u_k = 0.8$ . These values are substituted in (6a), and a numeric root-finding algorithm finds the unknown  $\theta_{k+1}$ . In this case, the Newton-Raphson method was used to find  $\theta_{k+1} = 0.2471$ . Finally, the updated discrete momentum is calculated using (6b):  $p_{k+1} = 0.3627$ . Computation of this example utilizing `trep` may be found at <https://trep.googlecode.com/git/examples/papers/tase2012/pend-single-step.py>. Note that it is already evident in this example that implicitly defined updates are to be expected. However, as we will see, these implicit updates have explicit linearizations that can be computed as functions of the configuration. Next we discuss the choice of state space for such a linearization.

## III. STATE SPACE FORM

In continuous time, the configuration and velocity of an Euler-Lagrange system are often concatenated into a single state  $x = [q \ \dot{q}]^T$  to create a first-order representation of the system. This choice cannot be easily used for the variational integrator because the finite-difference approximation of the velocity involves configurations at different time steps. Instead, the one-step representation of the integrator [1] in Eq. (2) suggests that for the variational integrator a convenient choice for the state is:

$$x_{k+1} = \begin{bmatrix} q_{k+1} \\ p_{k+1} \end{bmatrix} = f(x_k, u_k), \quad (7)$$

where the function  $f(x_k, u_k)$  is implicitly defined by Eq. (2). However, the Implicit Function Theorem guarantees that such a function exists provided that the derivative

$$M_{k+1} = D_2 D_1 L_{k+1} + D_2 F_{k+1}^- \quad (8)$$

is non-singular at  $q_k$ ,  $p_k$ , and  $u_k$ . This justifies abstracting the discrete dynamics of the variational integrator this way even though the underlying implementation still calculates the update  $q_{k+1}$  by numerically solving (2a). The purpose of this abstraction is to define the form for the linearization of the discrete dynamics. In the next section, we derive this linearization and find that the derivatives of the abstract  $f(x_k, u_k)$  representation are calculated explicitly.

## IV. FIRST DERIVATIVE

Analysis and optimal control methods often rely on the first-order linearization of system dynamics about a trajectory [5]. The first-order linearization of the discrete dynamics for the state form in Eq. (7) in Sec. III is:

$$\begin{aligned} \delta x_{k+1} &= \frac{\partial f}{\partial x_k} \delta x_k + \frac{\partial f}{\partial u_k} \delta u_k \\ \begin{bmatrix} \delta q_{k+1} \\ \delta p_{k+1} \end{bmatrix} &= \begin{bmatrix} \frac{\partial q_{k+1}}{\partial q_k} & \frac{\partial q_{k+1}}{\partial p_k} \\ \frac{\partial p_{k+1}}{\partial q_k} & \frac{\partial p_{k+1}}{\partial p_k} \end{bmatrix} \begin{bmatrix} \delta q_k \\ \delta p_k \end{bmatrix} + \begin{bmatrix} \frac{\partial q_{k+1}}{\partial u_k} \\ \frac{\partial p_{k+1}}{\partial u_k} \end{bmatrix} \delta u_k. \end{aligned} \quad (9)$$

Six components are required to calculate this linearization. These derivatives are found directly from the variational integrator equations (2), and all of them result in explicit equations.

Derivatives of  $q_{k+1}$  are found by implicitly differentiating (2a) and solving for the desired derivative. We start by finding  $\frac{\partial q_{k+1}}{\partial q_k}$ :

$$\begin{aligned} \frac{\partial}{\partial q_k} [p_k + D_1 L_{k+1} + F_{k+1}^- = 0] \\ 0 + D_1 D_1 L_{k+1} + D_2 D_1 L_{k+1} \frac{\partial q_{k+1}}{\partial q_k} + D_1 F_{k+1}^- \\ + D_2 F_{k+1}^- \frac{\partial q_{k+1}}{\partial q_k} = 0 \\ [D_2 D_1 L_{k+1} + D_2 F_{k+1}^-] \frac{\partial q_{k+1}}{\partial q_k} = - [D_1 D_1 L_{k+1} + D_1 F_{k+1}^-] \\ \frac{\partial q_{k+1}}{\partial q_k} = -M_{k+1}^{-1} [D_1 D_1 L_{k+1} + D_1 F_{k+1}^-] \end{aligned} \quad (10)$$

where  $M_{k+1}$  is as defined by (8) and is assumed to be non-singular (otherwise the Implicit Function Theorem would not apply, making the state representation invalid).

The process is repeated to calculate  $\frac{\partial q_{k+1}}{\partial p_k}$  and  $\frac{\partial q_{k+1}}{\partial u_k}$ :

$$\frac{\partial q_{k+1}}{\partial p_k} = -M_{k+1}^{-1} \quad (11)$$

$$\frac{\partial q_{k+1}}{\partial u_k} = -M_{k+1}^{-1} \cdot D_3 F_{k+1}^- \quad (12)$$

Notice that each of these derivatives depends on the new configuration  $q_{k+1}$  (e.g.,  $D_1 D_1 L_{k+1} = D_1 D_1 L_d(q_k, q_{k+1})$ ). Before evaluating the derivatives,  $q_{k+1}$  must be found by solving (2a).

Derivatives of  $p_{k+1}$  are found directly by differentiating (2b):

$$\frac{\partial p_{k+1}}{\partial q_k} = [D_2 D_2 L_{k+1} + D_2 F_{k+1}^+] \frac{\partial q_{k+1}}{\partial q_k} + D_1 D_2 L_{k+1} + D_1 F_{k+1}^+ \quad (13)$$

$$\frac{\partial p_{k+1}}{\partial p_k} = [D_2 D_2 L_{k+1} + D_2 F_{k+1}^+] \frac{\partial q_{k+1}}{\partial p_k} \quad (14)$$

$$\frac{\partial p_{k+1}}{\partial u_k} = [D_2 D_2 L_{k+1} + D_2 F_{k+1}^+] \frac{\partial q_{k+1}}{\partial u_k} + D_3 F_{k+1}^+ \quad (15)$$

These derivatives depend on (10)–(12), so (10)–(12) must be evaluated first. Once calculated, their values are used in (13)–(15) along with the known value of  $q_{k+1}$  to find the derivatives of  $p_{k+1}$ . Once all six derivatives are calculated, they are organized into the two matrices in (9) to get the complete first-order linearization about the current state. Lastly, note that the linearization is expressed entirely in terms of the discrete Lagrangian's dependence on the configuration and the discrete forcing function's dependence on the configuration and the continuous-time force. This is critical in understanding how to calculate the linearization without resorting to symbolic software, as discussed in Section VIII.

#### A. Example: Pendulum (cont.)

We continue the pendulum example from II-A by calculating the first linearization (again, at the initial conditions  $p_k = 0.5$ ,  $q_k = \theta_k = 0.2$ , with a timestep of  $\Delta t = 0.1$ , and an applied torque of  $u_k = 0.8$ ). The derivatives of the discrete Lagrangian  $L_d$  are:

$$\begin{aligned} D_1 D_1 L_d &= \frac{1}{\Delta t} - \frac{g\Delta t}{4} \cos \frac{\theta_{k+1} + \theta_k}{2} = 9.7610 \\ D_2 D_1 L_d &= -\frac{1}{\Delta t} - \frac{g\Delta t}{4} \cos \frac{\theta_{k+1} + \theta_k}{2} = -10.2389 \\ D_1 D_2 L_d &= -\frac{1}{\Delta t} - \frac{g\Delta t}{4} \cos \frac{\theta_{k+1} + \theta_k}{2} = -10.2389 \\ D_2 D_2 L_d &= \frac{1}{\Delta t} - \frac{g\Delta t}{4} \cos \frac{\theta_{k+1} + \theta_k}{2} = 9.7610. \end{aligned}$$

The derivatives of the discrete forcing are trivial:

$$\begin{aligned} D_1 F_d^- &= D_2 F_d^- = 0 \\ D_3 F_d^- &= \Delta t. \end{aligned}$$

Using these values with (8), we find  $M_{k+1}^{-1} = (-10.2389 + 0)^{-1} = -0.0976$ . These are used with (10)–(12) to calculate the derivatives of  $q_{k+1}$ :

$$\frac{\partial q_{k+1}}{\partial q_k} = 0.0976 \cdot (9.7610 + 0) = 0.9533$$

$$\frac{\partial q_{k+1}}{\partial p_k} = 0.0976$$

$$\frac{\partial q_{k+1}}{\partial u_k} = 0.0976 \cdot 0.01 = 0.00976.$$

These values are part of the linearization, but are also required to calculate the derivatives of  $p_{k+1}$  from (13)–(15).

$$\frac{\partial p_{k+1}}{\partial q_k} = (9.7610 + 0) \cdot 0.9533 + -10.2389 + 0 = -0.9333$$

$$\frac{\partial p_{k+1}}{\partial p_k} = (9.7610 + 0) \cdot 0.0976 = 0.9533$$

$$\frac{\partial p_{k+1}}{\partial u_k} = (9.7610 + 0) \cdot 0.00976 + 0 = 0.09533$$

The six values define the entire first-order linearization:

$$\delta x_{k+1} = \begin{bmatrix} 0.9533 & 0.0976 \\ -0.9333 & 0.9533 \end{bmatrix} \delta x_k + \begin{bmatrix} 0.00976 \\ 0.09533 \end{bmatrix} \delta u_k.$$

The first-order linearization frequently appears in analysis applications. For example, we can examine the controllability matrix of the pendulum at this configuration to verify that it is linearly controllable:

$$\begin{aligned} C = [B \quad AB] &= \begin{bmatrix} 0.00976 & 0.0186 \\ 0.09533 & 0.0818 \end{bmatrix} \\ \text{rank}(C) &= 2. \end{aligned}$$

This linearization is carried out using `trep` at <https://trep.googlecode.com/git/examples/papers/tase2012/pend-linearization.py>.

## V. SECOND DERIVATIVE

Optimal control applications can make use of the second-order linearization of the dynamics to improve their convergence rate [23]; this is illustrated in Sec. VIII-A. The approach used in Sec. IV extends to the second derivative of the dynamics as well (we will call this the second-order linearization). The expanded second-order linearization of the discrete dynamics is

$$\delta^2 x_{k+1} = \begin{bmatrix} \delta q_k \\ \delta p_k \\ \delta u_k \end{bmatrix}^T \begin{bmatrix} \frac{\partial^2 f}{\partial q_k \partial q_k} & \frac{\partial^2 f}{\partial q_k \partial p_k} & \frac{\partial^2 f}{\partial q_k \partial u_k} \\ \frac{\partial^2 f}{\partial p_k \partial q_k} & \frac{\partial^2 f}{\partial p_k \partial p_k} & \frac{\partial^2 f}{\partial p_k \partial u_k} \\ \frac{\partial^2 f}{\partial u_k \partial q_k} & \frac{\partial^2 f}{\partial u_k \partial p_k} & \frac{\partial^2 f}{\partial u_k \partial u_k} \end{bmatrix} \begin{bmatrix} \delta q_k \\ \delta p_k \\ \delta u_k \end{bmatrix}$$

where symmetry is used to reduce the number of unique entries in the  $3 \times 3$  array of third-order tensors to six. From Eq. (7) we have  $f = [q_{k+1} \ p_{k+1}]^T$ , so each derivative of  $f$  is calculated as two third-order tensor components; one for  $q_{k+1}$  and one for  $p_{k+1}$ . Thus 12 unique derivatives are needed for the second-order linearization.

### A. Derivatives of $q_{k+1}$

As with the first derivatives, the second derivatives of  $q_{k+1}$  are found by differentiating (2a) twice and solving for the desired derivative. We will be using the notation  $M \circ (X, Y)$  to represent a bilinear operator<sup>2</sup>  $M$  operating on  $X$  and  $Y$ . We find  $\frac{\partial^2 q_{k+1}}{\partial q_k \partial q_k}$  as an example:

$$\begin{aligned} \frac{\partial^2}{\partial q_k \partial q_k} [p_k + D_1 L_{k+1} + F_{k+1}^- = 0] \\ \frac{\partial}{\partial q_k} \left( [D_2 D_1 L_{k+1} + D_2 F_{k+1}^-] \frac{\partial q_{k+1}}{\partial q_k} = \right. \\ \left. - [D_1 D_1 L_{k+1} + D_1 F_{k+1}^-] \right) \end{aligned}$$

so we get that

$$\begin{aligned} [D_2 D_1 L_{k+1} + D_2 F_{k+1}^-] \frac{\partial^2 q_{k+1}}{\partial q_k \partial q_k} \\ + [D_1 D_2 D_1 L_{k+1} + D_1 D_2 F_{k+1}^-] \frac{\partial q_{k+1}}{\partial q_k} \\ + [D_2 D_2 D_1 L_{k+1} + D_2 D_2 F_{k+1}^-] \circ \left( \frac{\partial q_{k+1}}{\partial q_k}, \frac{\partial q_{k+1}}{\partial q_k} \right) \\ = - [D_1 D_1 D_1 L_{k+1} + D_1 D_1 F_{k+1}^-] \\ - [D_2 D_1 D_1 L_{k+1} + D_2 D_1 F_{k+1}^-] \frac{\partial q_{k+1}}{\partial q_k}. \end{aligned}$$

Solving for the desired derivative and substituting (8) we get

$$\begin{aligned} \frac{\partial^2 q_{k+1}}{\partial q_k \partial q_k} = -M_{k+1}^{-1} \left( [D_1 D_1 D_1 L_{k+1} + D_1 D_1 F_{k+1}^-] + \right. \\ \left. [D_1 D_2 D_1 L_{k+1} + D_1 D_2 F_{k+1}^-] + \right. \\ \left. D_2 D_1 D_1 L_{k+1} + D_2 D_1 F_{k+1}^- \right] \frac{\partial q_{k+1}}{\partial q_k} \\ + [D_2 D_2 D_1 L_{k+1} + D_2 D_2 F_{k+1}^-] \circ \left( \frac{\partial q_{k+1}}{\partial q_k}, \frac{\partial q_{k+1}}{\partial q_k} \right) \right) \quad (16) \end{aligned}$$

Previously we saw that the next state  $x_{k+1}$  had to be found in order to calculate the first derivatives. Here we see that the second derivative requires the first derivative as well. This establishes the required order for these calculations: The next state is found by the variational integrator, then that state is used to calculate the first derivative, and then both results are used to calculate the second derivative.

The other five second derivatives of  $q_{k+1}$  are found by the same procedure. The remaining derivatives with respect to state variables are:

$$\begin{aligned} \frac{\partial^2 q_{k+1}}{\partial q_k \partial p_k} = -M_{k+1}^{-1} \left( [D_2 D_1 D_1 L_{k+1} + D_2 D_1 F_{k+1}^-] \frac{\partial q_{k+1}}{\partial p_k} \right. \\ \left. + [D_2 D_2 D_1 L_{k+1} + D_2 D_2 F_{k+1}^-] \circ \left( \frac{\partial q_{k+1}}{\partial q_k}, \frac{\partial q_{k+1}}{\partial p_k} \right) \right) \quad (17) \end{aligned}$$

and

$$\begin{aligned} \frac{\partial^2 q_{k+1}}{\partial p_k \partial p_k} = \\ -M_{k+1}^{-1} [D_2 D_2 D_1 L_{k+1} + D_2 D_2 F_{k+1}^-] \circ \left( \frac{\partial q_{k+1}}{\partial p_k}, \frac{\partial q_{k+1}}{\partial p_k} \right). \quad (18) \end{aligned}$$

<sup>2</sup>This is equivalent to the matrix representation  $X^T M Y$  in finite dimensions, but this notation extends to infinite dimensional spaces such as those encountered in continuous trajectory optimization.

The derivatives with respect to state and input variables are:

$$\begin{aligned} \frac{\partial^2 q_{k+1}}{\partial q_k \partial u_k} = -M_{k+1}^{-1} \left( D_3 D_1 F_{k+1}^- + D_3 D_2 F_{k+1}^- \frac{\partial q_{k+1}}{\partial q_k} \right. \\ \left. + [D_2 D_1 D_1 L_{k+1} + D_2 D_1 F_{k+1}^-] \frac{\partial q_{k+1}}{\partial u_k} \right. \\ \left. + [D_2 D_2 D_1 L_{k+1} + D_2 D_2 F_{k+1}^-] \circ \left( \frac{\partial q_{k+1}}{\partial q_k}, \frac{\partial q_{k+1}}{\partial u_k} \right) \right) \quad (19) \end{aligned}$$

and

$$\begin{aligned} \frac{\partial^2 q_{k+1}}{\partial p_k \partial u_k} = -M_{k+1}^{-1} \left( D_3 D_2 F_{k+1}^- \frac{\partial q_{k+1}}{\partial p_k} \right. \\ \left. + [D_2 D_2 D_1 L_{k+1} + D_2 D_2 F_{k+1}^-] \circ \left( \frac{\partial q_{k+1}}{\partial p_k}, \frac{\partial q_{k+1}}{\partial u_k} \right) \right). \quad (20) \end{aligned}$$

The second derivative of the next configuration with respect to the inputs is:

$$\begin{aligned} \frac{\partial^2 q_{k+1}}{\partial u_k \partial u_k} = \\ -M_{k+1}^{-1} \left( D_3 D_3 F_{k+1}^- + [D_3 D_2 F_{k+1}^- + D_2 D_3 F_{k+1}^-] \frac{\partial q_{k+1}}{\partial u_k} \right. \\ \left. + [D_2 D_2 D_1 L_{k+1} + D_2 D_2 F_{k+1}^-] \circ \left( \frac{\partial q_{k+1}}{\partial u_k}, \frac{\partial q_{k+1}}{\partial u_k} \right) \right). \quad (21) \end{aligned}$$

These six derivatives make up the entire second linearization of the first half of the state.

1) *Pendulum (cont.)*: We now return to the pendulum example, again with the same initial data. We calculate the first part of the second-order linearization directly from (16)–(21). The next state and first-order linearization of the pendulum were already found in Sec. II-A and IV-A, respectively. After calculating the higher derivatives of  $L_{k+1}$  and  $F_{k+1}^\pm$ , we find the second derivative of the pendulum's configuration dynamics  $\delta^2 q_{k+1} =$

$$\begin{bmatrix} \delta q_k \\ \delta p_k \\ \delta u_k \end{bmatrix}^T \begin{bmatrix} 1.01 \times 10^{-2} & 5.06 \times 10^{-4} & 5.06 \times 10^{-5} \\ 5.06 \times 10^{-4} & 2.53 \times 10^{-5} & 2.53 \times 10^{-6} \\ 5.06 \times 10^{-5} & 2.53 \times 10^{-6} & 2.53 \times 10^{-7} \end{bmatrix} \begin{bmatrix} \delta q_k \\ \delta p_k \\ \delta u_k \end{bmatrix}.$$

We also need the second derivatives of  $p_{k+1}$  to complete the second-order linearization.

### B. Derivatives of $p_{k+1}$

The six derivatives of the momentum component of the state,  $p_{k+1}$  are calculated directly from the explicit momentum equation (2b). The derivatives with respect to state variables are:

$$\begin{aligned} \frac{\partial^2 p_{k+1}}{\partial q_k \partial q_k} = D_1 D_1 D_2 L_{k+1} + D_1 D_1 F_{k+1}^+ \\ + [D_2 D_2 L_{k+1} + D_2 F_{k+1}^+] \frac{\partial^2 q_{k+1}}{\partial q_k \partial q_k} \\ + [D_2 D_1 D_2 L_{k+1} + D_1 D_2 D_2 L_{k+1} + \\ D_2 D_1 F_{k+1}^+ + D_1 D_2 F_{k+1}^+] \frac{\partial q_{k+1}}{\partial q_k} \\ + [D_2 D_2 D_2 L_{k+1} + D_2 D_2 F_{k+1}^+] \circ \left( \frac{\partial q_{k+1}}{\partial q_k}, \frac{\partial q_{k+1}}{\partial q_k} \right) \quad (22) \end{aligned}$$

$$\begin{aligned} \frac{\partial^2 p_{k+1}}{\partial q_k \partial p_k} = [D_2 D_1 D_2 L_{k+1} + D_2 D_1 F_{k+1}^+] \frac{\partial q_{k+1}}{\partial p_k} \\ + [D_2 D_2 L_{k+1} + D_2 F_{k+1}^+] \frac{\partial^2 q_{k+1}}{\partial q_k \partial p_k} \\ + [D_2 D_2 D_2 L_{k+1} + D_2 D_2 F_{k+1}^+] \circ \left( \frac{\partial q_{k+1}}{\partial q_k}, \frac{\partial q_{k+1}}{\partial p_k} \right) \quad (23) \end{aligned}$$

$$\begin{aligned} \frac{\partial^2 p_{k+1}}{\partial p_k \partial p_k} &= [D_2 D_2 L_{k+1} + D_2 F_{k+1}^+] \frac{\partial^2 q_{k+1}}{\partial p_k \partial p_k} \\ &+ [D_2 D_2 D_2 L_{k+1} + D_2 D_2 F_{k+1}^+] \circ \left( \frac{\partial q_{k+1}}{\partial p_k}, \frac{\partial q_{k+1}}{\partial p_k} \right). \end{aligned} \quad (24)$$

The derivatives with respect to state and input variables are:

$$\begin{aligned} \frac{\partial^2 p_{k+1}}{\partial q_k \partial u_k} &= D_3 D_1 F_{k+1}^+ + D_3 D_2 F_{k+1}^+ \frac{\partial q_{k+1}}{\partial q_k} + [D_2 D_1 D_2 L_{k+1} \\ &+ D_2 D_1 F_{k+1}^+] \frac{\partial q_{k+1}}{\partial u_k} + [D_2 D_2 L_{k+1} + D_2 F_{k+1}^+] \frac{\partial^2 q_{k+1}}{\partial q_k \partial u_k} \\ &+ [D_2 D_2 D_2 L_{k+1} + D_2 D_2 F_{k+1}^+] \circ \left( \frac{\partial q_{k+1}}{\partial q_k}, \frac{\partial q_{k+1}}{\partial u_k} \right) \end{aligned} \quad (25)$$

$$\begin{aligned} \frac{\partial^2 p_{k+1}}{\partial p_k \partial u_k} &= D_3 D_2 F_{k+1}^+ \frac{\partial q_{k+1}}{\partial p_k} + \\ &[D_2 D_2 L_{k+1} + D_2 F_{k+1}^+] \frac{\partial^2 q_{k+1}}{\partial p_k \partial u_k} \\ &+ [D_2 D_2 D_2 L_{k+1} + D_2 D_2 F_{k+1}^+] \circ \left( \frac{\partial q_{k+1}}{\partial p_k}, \frac{\partial q_{k+1}}{\partial u_k} \right). \end{aligned} \quad (26)$$

Finally, the second derivative with respect to the input variables is:

$$\begin{aligned} \frac{\partial^2 p_{k+1}}{\partial u_k \partial u_k} &= D_3 D_3 F_{k+1}^+ + [D_3 D_2 F_{k+1}^+ + D_2 D_3 F_{k+1}^+] \frac{\partial q_{k+1}}{\partial u_k} \\ &+ [D_2 D_2 D_2 L_{k+1} + D_2 D_2 F_{k+1}^+] \circ \left( \frac{\partial q_{k+1}}{\partial u_k}, \frac{\partial q_{k+1}}{\partial u_k} \right) \\ &+ [D_2 D_2 L_{k+1} + D_2 F_{k+1}^+] \frac{\partial^2 q_{k+1}}{\partial u_k \partial u_k}. \end{aligned} \quad (27)$$

As with the first derivatives, the second derivatives of  $p_{k+1}$  depend on those of  $q_{k+1}$ . We handle this dependency by first evaluating (16)–(21) to get their numerical values and then plug those values into (22)–(27).

**Note:** By evaluating each of the twelve equations above, we explicitly calculate the complete second-order linearization for a forced system in generalized coordinates. Section VI describes how this approach is extended to systems with holonomic constraints.

1) *Pendulum (cont.):* We complete the second derivative by evaluating (22)–(27) with the values found earlier and the remaining derivatives of  $L_{k+1}$  and  $F_{k+1}^\pm$ . The result is  $\delta^2 p_{k+1} =$

$$\begin{bmatrix} \delta q_k \\ \delta p_k \\ \delta u_k \end{bmatrix}^T \begin{bmatrix} 2.02 \times 10^{-1} & 1.01 \times 10^{-2} & 1.01 \times 10^{-3} \\ 1.01 \times 10^{-2} & 5.06 \times 10^{-4} & 5.06 \times 10^{-5} \\ 1.01 \times 10^{-3} & 5.06 \times 10^{-5} & 5.06 \times 10^{-6} \end{bmatrix} \begin{bmatrix} \delta q_k \\ \delta p_k \\ \delta u_k \end{bmatrix}.$$

These second-order linearizations  $\delta^2 q_{k+1}$  and  $\delta^2 p_{k+1}$  carried out using `trep` can be found at <https://trep.googlecode.com/git/examples/papers/tase2012/pend-linearization.py>.

## VI. CONSTRAINED SYSTEMS

In this section, we discuss how the approach described in Sec. IV and V to calculate the discrete linearizations extends to constrained variational integrators. Variational integrators are particularly well-suited to systems with holonomic constraints because the update equation for a constrained variational integrator explicitly incorporates the holonomic constraint. This is opposed to replacing the holonomic constraint with its derivatives and then projecting the update onto the feasible set, a common approach in numeric integration of ordinary

differential equations. Variational integrators enforce the holonomic constraint at every time step while still preserving the symplectic form and conserving momentum.

Variational integrators for constrained systems [21] are derived using the same Lagrange-multiplier method used in the continuous case [22]. Given a continuous-time constraint of the form  $h(q) = 0$ , the DEL equations for a forced, constrained variational integrator are:

$$p_k + D_1 L_{k+1} + F_{k+1}^- - Dh^T(q_k) \lambda_k = 0 \quad (28a)$$

$$h(q_{k+1}) = 0 \quad (28b)$$

$$p_{k+1} = D_2 L_{k+1} + F_{k+1}^+ \quad (28c)$$

where  $\lambda_k$  are the Lagrange multipliers that can be interpreted as discrete-time forces enforcing the constraint. In this case, given  $p_k$  and  $q_k$ , a root-finding algorithm solves (28a) and (28b) to find  $q_{k+1}$  and  $\lambda_k$ . The updated momentum  $p_{k+1}$  is then explicitly calculated from (28c).

The Lagrange multipliers are completely determined by  $q_k$ ,  $p_k$ , and  $u_k$ , so the state representation from Section III is unchanged. Accordingly, the same derivatives  $\delta x_{k+1}$  and  $\delta^2 x_{k+1}$  are needed to find the linearizations. Rather than derive every equation, we calculate one component of the first and second derivatives to demonstrate the process.

For the first-order linearization, we find  $\frac{\partial q_{k+1}}{\partial q_k}$ . We start by differentiating (28a):

$$\begin{aligned} \frac{\partial}{\partial q_k} [p_k + D_1 L_{k+1} + F_{k+1}^- - Dh^T(q_k) \lambda_k = 0] \\ \Rightarrow \frac{\partial q_{k+1}}{\partial q_k} = -M_k^{-1} \left[ C_{q_k} - Dh^T(q_k) \frac{\partial \lambda_k}{\partial q_k} \right] \end{aligned} \quad (29)$$

where

$$C_{q_k} = D_1 D_1 L_{k+1} + D_1 F_{k+1}^- - D^2 h^T(q_k) \lambda_k.$$

To evaluate this derivative, we must calculate  $\frac{\partial \lambda_k}{\partial q_k}$ . This is found by differentiating (28b), substituting in (29), and solving for  $\frac{\partial \lambda_k}{\partial q_k}$ :

$$\begin{aligned} \frac{\partial}{\partial q_k} [h(q_{k+1}) = 0] \\ Dh(q_{k+1}) \frac{\partial q_{k+1}}{\partial q_k} = 0 \\ Dh(q_{k+1}) M_k^{-1} \left[ C_{q_k} - Dh^T(q_k) \frac{\partial \lambda_k}{\partial q_k} \right] = 0 \\ Dh(q_{k+1}) M_k^{-1} C_{q_k} - Dh(q_{k+1}) M_k^{-1} Dh^T(q_k) \frac{\partial \lambda_k}{\partial q_k} = 0 \\ \frac{\partial \lambda_k}{\partial q_k} = [Dh(q_{k+1}) M_k^{-1} Dh^T(q_k)]^{-1} Dh(q_{k+1}) M_k^{-1} C_{q_k}. \end{aligned} \quad (30)$$

To calculate  $\frac{\partial q_{k+1}}{\partial q_k}$ , the constrained DEL equation (28) is solved numerically to find  $q_{k+1}$  and  $\lambda_k$ . These values are used in (30) to find  $\frac{\partial \lambda_k}{\partial q_k}$ . Finally,  $\frac{\partial q_{k+1}}{\partial q_k}$  is calculated with (29).

The same approach is used to find the remaining components of the first derivative, so we do not repeat the derivation here. Derivations of the remaining components can be found in [24]. We continue onto the second derivative by calculating  $\frac{\partial^2 q_{k+1}}{\partial q_k \partial q_k}$ .

$$\begin{aligned} \frac{\partial^2}{\partial q_k \partial q_k} [p_k + D_1 L_{k+1} + F_{k+1}^- - Dh^T(q_k) \lambda_k = 0] \\ \Rightarrow \frac{\partial^2 q_{k+1}}{\partial q_k \partial q_k} = -M_{k+1}^{-1} \left( C_{q_k q_k} - Dh^T(q_k) \frac{\partial^2 \lambda_k}{\partial q_k \partial q_k} \right) \end{aligned} \quad (31)$$

where

$$\begin{aligned}
C_{q_k q_k} = & D_1 D_1 D_1 L_{k+1} + D_1 D_1 F_{k+1}^- \\
& + \left[ D_2 D_1 D_1 L_{k+1} + D_2 D_1 F_{k+1}^- \right. \\
& \quad \left. + D_1 D_2 D_1 L_{k+1} + D_1 D_2 F_{k+1}^- \right] \frac{\partial q_{k+1}}{\partial q_k} \\
& + \left[ D_2 D_2 D_1 L_{k+1} + D_2 D_2 F_{k+1}^- \right] \circ \left( \frac{\partial q_{k+1}}{\partial q_k}, \frac{\partial q_{k+1}}{\partial q_k} \right) \\
& - D^3 h^T(q_k) \lambda_k - 2D^2 h^T(q_k) \frac{\partial \lambda_k}{\partial q_k}.
\end{aligned}$$

Again, we find the corresponding second derivative of  $\lambda_k$  by differentiating (28b) twice:

$$D^2 h(q_{k+1}) \circ \left( \frac{\partial q_{k+1}}{\partial q_k}, \frac{\partial q_{k+1}}{\partial q_k} \right) + Dh(q_{k+1}) \frac{\partial^2 q_{k+1}}{\partial q_k \partial q_k} = 0.$$

We substitute in (31) and solve for  $\frac{\partial^2 \lambda_k}{\partial q_k \partial q_k}$ :

$$\begin{aligned}
\frac{\partial^2 \lambda_k}{\partial q_k \partial q_k} = & [Dh(q_{k+1}) M_{k+1}^{-1} Dh^T(q_k)] \cdot \\
& \left[ Dh(q_{k+1}) M_{k+1}^{-1} C_{q_k q_k} - D^2 h(q_{k+1}) \circ \left( \frac{\partial q_{k+1}}{\partial q_k}, \frac{\partial q_{k+1}}{\partial q_k} \right) \right]. \quad (32)
\end{aligned}$$

To calculate this  $\frac{\partial^2 q_{k+1}}{\partial q_k \partial q_k}$ , we solve for the next state, calculate the first derivatives, evaluate (32) to find  $\frac{\partial^2 \lambda_k}{\partial q_k \partial q_k}$ , and finally evaluate (31) to find the second derivative. This same procedure is used to calculate the other components of the constrained second derivative.

Note that the constrained momentum update (28c) is identical to the unconstrained case (2b), so the first- and second-order linearizations are identical.

## VII. SINGULARITIES OF THE LINEARIZATION

Eq. (8) includes a matrix  $M_{k+1}$  that must be inverted in both the first and second order linearizations presented in Sec. IV and Sec. V respectively. Additionally Sec. VI shows that when the system involves constraints, the linearizations additionally involve the term  $[Dh(q_{k+1}) M_k^{-1} Dh^T(q_k)]^{-1}$ . For a general mechanical system, the requirements for invertibility of these two terms are not known, but certainly the choice of coordinate chart can cause singularities as can degeneracy of the Lagrangian system. We illustrate this point by presenting two simple examples that demonstrate situations where  $M_{k+1}$  and  $[Dh(q_{k+1}) M_k^{-1} Dh^T(q_k)]$  become singular.

### A. Singularities of $M_{k+1}$ in a Spherical Pendulum

Consider an unforced, spherical pendulum of mass  $m$  and length  $r$  under the influence of gravity  $g$  in generalized coordinates  $q = (\theta, \phi)$  where  $\theta$  is the polar angle measured from the zenith direction which is aligned with gravity, and  $\phi$  is the azimuthal angle. For this system, the Lagrangian is given by

$$L(q, \dot{q}) = \frac{1}{2} m r^2 (\dot{\theta}^2 + \sin^2 \theta \dot{\phi}^2) + mgr \cos \theta.$$

It is well-known that this choice of generalized coordinates does not provide a global chart, resulting in singular configurations. This can be seen by looking at the mass matrix for this system which is given by

$$M(q) = \frac{\partial^2 L}{\partial \dot{q} \partial \dot{q}} = \begin{bmatrix} m r^2 \sin^2(\theta) & 0 \\ 0 & m r^2 \end{bmatrix}. \quad (33)$$

Clearly this matrix is singular if  $\theta = n\pi \forall n \in \mathbb{Z}$  where  $\mathbb{Z}$  is the set of all integers. Using the midpoint-rule discrete Lagrangian of (3a) we can construct the discrete Lagrangian for this system as

$$\begin{aligned}
L_d(q_k, q_{k+1}) = & \frac{m r^2}{2} \left( \frac{\theta_{k+1} - \theta_k}{\Delta t} \right)^2 + \\
& \frac{m r^2}{2} \sin^2 \left( \frac{\theta_{k+1} + \theta_k}{2} \right) \left( \frac{\phi_{k+1} - \phi_k}{\Delta t} \right)^2 + mgr \cos \left( \frac{\theta_{k+1} + \theta_k}{2} \right).
\end{aligned}$$

From (8)  $M_{k+1}$  may be calculated as

$$M_{k+1} = \begin{bmatrix} \frac{\partial^2 L_{k+1}}{\partial \phi_{k+1} \partial \phi_k} & \frac{\partial^2 L_{k+1}}{\partial \theta_{k+1} \partial \phi_k} \\ \frac{\partial^2 L_{k+1}}{\partial \phi_{k+1} \partial \theta_k} & \frac{\partial^2 L_{k+1}}{\partial \theta_{k+1} \partial \theta_k} \end{bmatrix}.$$

To find singularities of this matrix, set its determinant equal to zero. The determinant of  $M_{k+1}$  is

$$\begin{aligned}
\det(M_{k+1}) = & \frac{m^2 r^3}{4 \Delta t^2} \sin^2 \left( \frac{\theta_{k+1} + \theta_k}{2} \right) \left[ \Delta t^2 g \cos \left( \frac{\theta_{k+1} + \theta_k}{2} \right) \right. \\
& \left. + r(2 + \cos(\theta_{k+1} + \theta_k)) (\phi_k - \phi_{k+1})^2 + 4r \right]. \quad (34)
\end{aligned}$$

If the term before the brackets is zero then  $\det(M_{k+1}) = 0$  and the matrix is singular. This implies  $M_{k+1}$  is singular if  $\theta_{k+1} + \theta_k = n\pi \forall n \in \mathbb{Z}$ . Thus if the discrete system is at the singular configuration of the continuous system for two consecutive timesteps or if the consecutive configurations are symmetric about the singular configuration, then  $M_{k+1}$  is non-invertible.

Equation (34) is also zero if the term in the brackets is zero, implying that there exist sets of consecutive configurations that cause  $M_{k+1}$  to be singular that are not directly related to the continuous-time singular configurations. However, there exists an upper bound on the timestep size  $\Delta t$  that prevents the bracketed term from being zero. To illustrate, assume that the spherical pendulum is in pure pendular motion i.e.  $\phi_{k+1} = \phi_k$ . With this assumption setting the bracketed term to zero yields

$$\begin{aligned}
\Delta t^2 g \cos \left( \frac{\theta_{k+1} + \theta_k}{2} \right) + 4r = 0 \\
\implies \theta_{k+1} + \theta_k = 2 \cos^{-1} \left( \frac{-4r}{\Delta t^2 g} \right).
\end{aligned}$$

The inverse cosine is only defined if its argument  $\frac{-4r}{\Delta t^2 g} \in [-1, 1]$ . Noting that  $g$ ,  $r$ , and  $\Delta t$  are all greater than zero, we see that the argument is bounded above by zero. Thus the inverse cosine only has a solution if

$$\begin{aligned}
-1 \leq \frac{-4r}{\Delta t^2 g} \\
\implies \Delta t \geq \sqrt{\frac{4r}{g}}.
\end{aligned}$$



Thus if  $\Delta t < \sqrt{(4r)/g}$  and  $\phi_{k+1} = \phi_k$  the bracketed term is always nonzero and the only singularity that exists in  $M_{k+1}$  is the one induced by our choice of generalized coordinates.

If we relax the constraint  $\phi_{k+1} = \phi_k$  similar reasoning shows that for a given set of constants  $g$ ,  $r$ , and  $\Delta t$  then there exists an upper bound,  $\lambda^*$ , on the difference in  $\phi$  across a timestep such that if  $|\phi_k - \phi_{k+1}| \leq \lambda^*$  then the bracketed term cannot be zero. Thus for a given spherical pendulum, as long as the timestep is small enough, the only singularities that exist in  $M_{k+1}$  are singularities that are caused by the choice of generalized coordinates.

This example illustrates that singularities caused by a poor choice of local, generalized coordinates can show up as singularities in  $M_{k+1}$ . Additionally, other singularities in  $M_{k+1}$  can be related to coarse sampling of the continuous system and can be prevented by decreasing the mesh size.

### B. Singularities of a Constrained Pendulum

Consider again a simple pendulum system as shown in Fig. 2. Assume that gravity is zero. In this example, we will represent the system in Cartesian coordinates  $q = (x, y)$ , and we will add a constraint of the form

$$h(q) = x^2 + y^2 - l^2 = 0.$$

This system's midpoint discrete Lagrangian is

$$L_d(q_k, q_{k+1}) = \frac{1}{2}m \left( \left( \frac{x_{k+1} - x_k}{\Delta t} \right)^2 + \left( \frac{y_{k+1} - y_k}{\Delta t} \right)^2 \right).$$

We calculate  $M_{k+1}$  as

$$M_{k+1} = \begin{bmatrix} \frac{\partial^2 L_{k+1}}{\partial x_{k+1} \partial x_k} & \frac{\partial^2 L_{k+1}}{\partial y_{k+1} \partial x_k} \\ \frac{\partial^2 L_{k+1}}{\partial x_{k+1} \partial y_k} & \frac{\partial^2 L_{k+1}}{\partial y_{k+1} \partial y_k} \end{bmatrix} = \begin{bmatrix} \frac{-m}{\Delta t^2} & 0 \\ 0 & \frac{-m}{\Delta t^2} \end{bmatrix}$$

and see that it is always invertible. In order to linearize this system  $[Dh(q_{k+1})M_k^{-1}Dh^T(q_k)]$  must be invertible. Using the given  $h(q)$

$$[Dh(q_{k+1})M_k^{-1}Dh^T(q_k)] = -\frac{4\Delta t^2}{m}(x_{k+1}x_k + y_{k+1}y_k).$$

This is only non-invertible if  $Dh(q_k)$  and  $Dh(q_{k+1})$  are orthogonal in the Euclidean sense. This orthogonality would require the pendulum to move  $\pi/2$  rad in a single timestep. Regardless of how fast the pendulum is moving, we are guaranteed that as  $\Delta t \rightarrow 0$  the change in configuration goes to zero i.e.  $\|q_k - q_{k+1}\| \rightarrow 0$ . Thus there is always a sufficiently small timestep to ensure  $[Dh(q_{k+1})M_k^{-1}Dh^T(q_k)]$  is non-singular. From this example, it is clear that for a general mechanical system, even in cases where  $M_k$  is non-singular there may be situations where the term  $[Dh(q_{k+1})M_k^{-1}Dh^T(q_k)]$  may be singular.

Generalizing the ways in which a linearization of a variational integrator can cease to be well-posed is clearly an important issue to pursue. However, for purposes of a numerical method, it suffices to check that  $M_k$  and  $[Dh(q_{k+1})M_k^{-1}Dh^T(q_k)]$  are invertible at every time step to be confident that the computed linearization is correct.

## VIII. IMPLEMENTATION

Deriving the first- and second-order derivative equations of Sec. IV and V is procedurally straightforward. The more complicated issue in implementing the first- and second-order derivatives is calculating higher derivatives of the discrete Lagrangian and discrete forces. Approaches relying on the symbolic equations, as was done for the pendulum example, do not scale to complex systems even with the help of symbolic algebra software.

In [8], the authors describe a method to implement variational integrators using a hierarchical tree representation [25]–[27]. That approach calculates exact derivatives of the discrete Lagrangian numerically and scales to large, complex mechanical systems like a biomechanical model of the human hand [28]. Moreover, it calculates the derivatives of the discrete Lagrangian without ever having an explicit representation of the discrete Lagrangian itself; all the calculations are implicitly defined in terms of the tree representation that encodes the mechanical topology.

It should be noted that *how* one uses the mechanical topology to compute derivatives is not critical for the present work. Indeed, one could use any method that allows one to compute higher-order derivatives of the discrete Lagrangian (e.g., a spatial-operator approach [29] or a recursive dynamics [30] approach). So long as the computational method provides the derivatives from Section IV and V, the only risk is that one method may provide better or worse scaling properties than another method, something that is beyond the scope of the present paper.

The method in [8] naturally extends to calculating higher-order derivatives [17] of the discrete Lagrangian and discrete forcing that are needed by the first- and second-order linearizations [31]. Thus it provides a complete framework for implementing variational integrators and their first- and second-order linearizations.

These algorithms have been implemented in an open source software library called `trep`. The software calculates continuous and discrete dynamics, along with their first- and second-order linearizations, for arbitrary mechanical systems in generalized coordinates, including those with holonomic constraints. `trep` is freely available at <http://trep.googlecode.com>.

The following examples demonstrate the application of the first-order linearization as a tool for generating stabilizing controllers; the first example considers a simple pendulum, and the second features a more complex mechanical system highlighting the scalability of the method described in [8]. Additionally, the first example utilizes a second-order optimization technique requiring the second-order linearization presented in Sec. V. All of the calculations were performed by `trep`.

### A. Example: Optimal Control of the Pendulum

As a simple example, we once again consider the pendulum in Fig. 2. Using the choice of state discussed in Sec. III the state for this system is  $x(k) = [q(k) \ p(k)]^T$ . Here we are

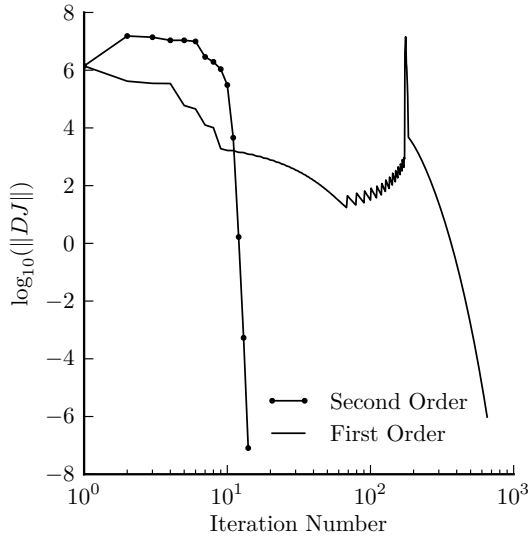


Fig. 3. Convergence rate of a first-order and a second-order optimization method for the pendulum example. The second order method converges to  $10^{-6}$  in 14 iterations while the first order method converges to the same tolerance after 653 iterations. On an Intel i7-3770K CPU at 3.50GHz descent direction computation requires, on average, 28.5 ms for the first-order method and 55.8 ms for the second-order method resulting in the second-order optimization converging in approximately 4% of the time required for the first-order optimization.

dropping the shortcut of using a subscript  $k$  to indicate sequence index to avoid confusion with other subscripts used for distinguishing trajectories. We begin by defining a dynamically infeasible, discrete reference trajectory over the time horizon  $t_{ref} = \{t_{ref}(k) = k\Delta t \mid k = 0, \dots, N\}$  with  $\Delta t = 0.1s$  and  $N = 100$  as

$$q_{ref} = \left\{ q_{ref}(k) = \begin{cases} 0 & \text{if } k \in [0, N/2) \\ \pi & \text{if } k \in [N/2, N] \end{cases} \right\} \quad (35a)$$

$$p_{ref} = \{p_{ref}(k) = 0 \mid k = 0, \dots, N\} \quad (35b)$$

$$u_{ref} = \{u_{ref}(k) = 0 \mid k = 0, \dots, N\}. \quad (35c)$$

Thus the reference trajectory is a step-function from the pendulum's stable equilibrium to its unstable equilibrium. It is clearly infeasible as the desired momentum term is zero for all time while the configuration is not, and the desired input is zero while the system moves away from an equilibrium.

An optimization routine is utilized to generate a dynamically feasible reference trajectory where the cost function includes a weighted running cost on state and input error as well as a weighted error of the final state. This optimization is performed using both a first-order method and a second-order method. The convergence of these two optimizations can be seen in Fig. 3 which illustrates the vastly increased convergence rate of the second-order method. Both methods converge to the same feasible trajectory. It is important to note that the second-order method requires the second derivatives presented in Sec. V.

Once the optimization is complete, we have a dynamically feasible desired trajectory given by  $x_d = \{x_d(k)\}_{k=0}^N$  and  $u_d = \{u_d(k)\}_{k=0}^{N-1}$ . We now linearize the system about the desired trajectory  $(x_d, u_d)$  using the derivatives of Sec. IV and then solve a Linear Quadratic Regulator (LQR) problem to find a controller that stabilizes the system about this desired

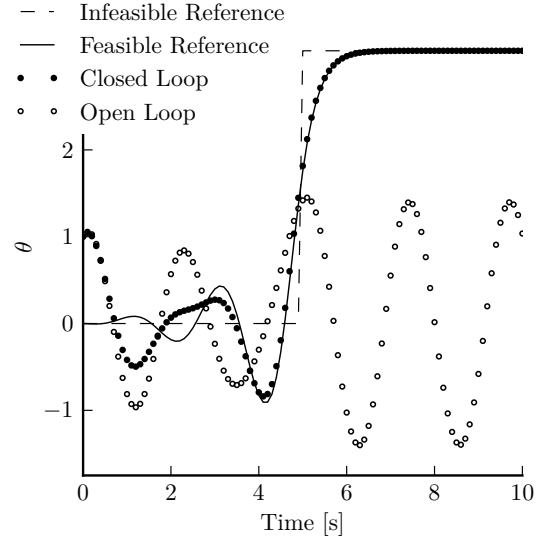


Fig. 4. Figure showing the performance of the LQR regulator for the pendulum example. The Infeasible Reference is the  $q_{ref}$  of (35a), the Feasible Reference is the desired trajectory found by the second-order optimization routine, the Closed Loop trajectory is produced by simulating the perturbed initial condition using (37), and the Open Loop trajectory uses the perturbed initial conditions with no stabilizing feedback.

trajectory [5]. The LQR problem for a discrete nonlinear system that has been linearized about a desired trajectory  $(x(k), u(k))$  seeks to find a control input  $\mu(k)$  that minimizes the quadratic cost

$$V(z_{k_0}, \mu(\cdot), k_0) = \sum_{k=k_0}^{k_f-1} [z^T(k)Q(k)z(k) + \mu^T(k)R(k)\mu(k)] + z^T(k_f)Q(k_f)z(k_f)$$

where

$$\begin{aligned} R(k) &= R^T(k) \geq 0 \quad \forall k \in \{k_0 \dots (k_f - 1)\} \\ Q(k) &= Q^T(k) \geq 0 \quad \forall k \in \{k_0 \dots k_f\} \\ z_{k_0} &= z_0 \\ z(k+1) &= A(k)z(k) + B(k)\mu(k) \end{aligned}$$

where  $z(k)$  and  $\mu(k)$  are perturbations from the desired trajectory [5]. The linearizations are  $A(k) = \frac{\partial f(x(k), u(k))}{\partial x(k)}$  and  $B(k) = \frac{\partial f(x(k), u(k))}{\partial u(k)}$ . The solution to this discrete LQR problem is found by solving the discrete Ricatti equation:

$$P(k) = Q(k) + A^T(k)P(k+1)A(k) - \quad (36a)$$

$$A^T(k)P(k+1)B(k)[R(k) + B^T(k)P(k+1)B(k)]^{-1} B^T(k)P(k+1)A(k)$$

$$P_{k_f} = Q_{k_f}. \quad (36b)$$

The Ricatti equation is solved to find  $P(k)$  by recursively evaluating (36a) backwards in time from the boundary condition (36b). The solution is used to calculate a feedback law:

$$\mathcal{K}(k) = [R(k) + B^T(k)P(k+1)B(k)]^{-1} B^T(k)P(k+1)B(k).$$

Using this feedback law with the original desired trajectory  $(x_d, u_d)$  yields the closed-loop system

$$\begin{aligned} x(0) &= x_0 \\ x(k+1) &= f(x(k), \bar{u}(k)) \\ \bar{u}(k) &= u_d(k) - \mathcal{K}(k)(x(k) - x_d(k)). \end{aligned} \quad (37)$$

To illustrate the stabilization of the controller obtained by solving the LQR problem we perturb the initial condition of the original optimization  $x_d(0) = [0 \ 0]^T$  to give an initial condition of  $x(0) = [1 \ 1]^T$  and then simulate the closed loop system of (37) with the perturbed initial condition. We also simulate the perturbed initial condition with no feedback. The results are shown in Fig. 4, and it can be seen that the feedback quickly stabilizes the closed-loop system to the feasible reference.

The optimization for generating a feasible trajectory using `trep` can be found at <https://trep.googlecode.com/git/examples/papers/tase2012/pend-optimization.py> and the simulations of the perturbed initial conditions can be found at <https://trep.googlecode.com/git/examples/papers/tase2012/pend-closed-loop.py>.

### B. Example: Marionette

As more complex example, we again use the Linear Quadratic Regulator (LQR) method to generate a stabilizing feedback controller for the mechanical marionette in Fig. 5. The marionette has 22 dynamic configuration variables, 18 kinematic configuration variables [32], and 6 holonomic constraints. The corresponding state-space model has 80 state and 18 input variables.

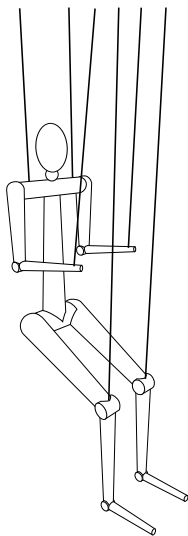


Fig. 5. The marionette model has 40 configuration variables and 6 holonomic constraints.

The marionette was simulated and linearized about a 10.0 second trajectory using the midpoint variational integrator in `trep`. The reference trajectory was generated by changing the string lengths of the arms and legs using  $\pm 0.1 \sin(0.6\pi t)$  input

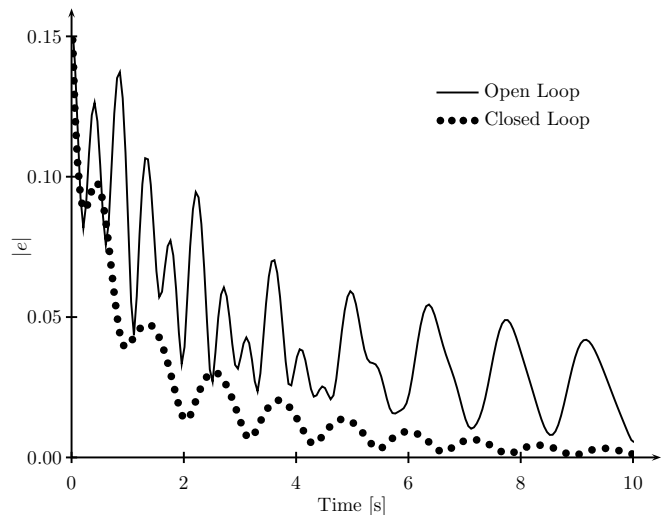


Fig. 6. The discrete LQR feedback law significantly improves the norm of the error response of the marionette compared to the open-loop simulation.

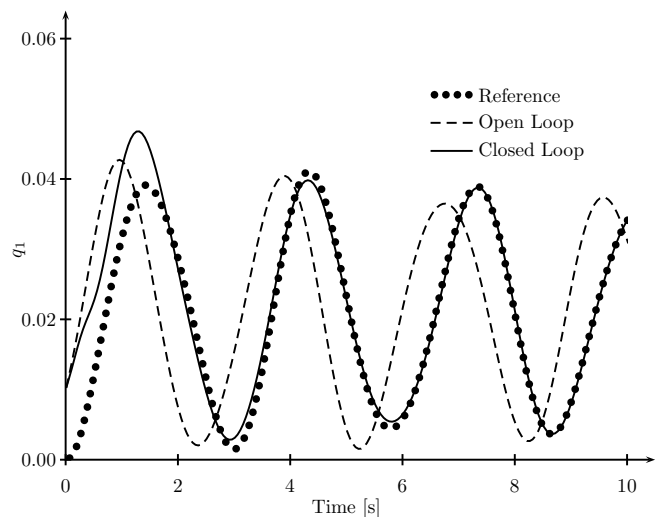


Fig. 7. The discrete LQR feedback law also significantly improves the individual error response of the marionette compared to the open-loop simulation. This is the trajectory of the configuration of the vertical orientation of the torso.

signals. The linearization was used to create a locally stabilizing controller by solving the discrete LQR problem with diagonal matrices for each cost matrix with an entry of 100 for the configuration variables and identity everywhere else. A perturbation of  $0.1 \text{ rad}$  was then added to the initial condition of the vertical orientation of the torso and the simulation was performed with and without the added stabilizing feedback controller.

The norm of the resulting error between the perturbed and original trajectories is shown in Fig. 6 and the trajectory of the vertical orientation of the torso is shown in Fig. 7 as an example of stabilization of one of the states. As expected, the closed-loop trajectory quickly converges to the reference trajectory while the errors in the open-loop trajectory persist throughout the time horizon. The ability to generate locally stabilizing feedback laws for complex systems that are simu-

lated with variational integrators is a useful application of the methods described here. The source code for this example can be obtained at <https://trep.googlecode.com/git/examples/papers/tase2012/marionette.py>.

The optimization was performed on an Intel i7-2760QM CPU at 2.40GHz. The simulation takes approximately 2.11 ms per step, the linearization takes approximately 1.12 ms per step. The second-order linearization takes approximately 22.15 ms per step, though it was not required for this example.

## IX. CONCLUSION

Variational integrators are an appealing alternative to numerically integrating continuous equations of motion. By representing variational integrators as discrete dynamic systems and calculating the linearization of the associated one-step map, their utility is extended to applications requiring analysis and optimal control. This approach reduces complexity, potential for error, and extraneous work compared to using a variational integrator for simulation while doing the analysis and optimization in the continuous domain with a separate set of equations. Moreover, it leads to feedback laws that are expressed purely in terms of configuration variables (instead of configurations and configuration velocities).

The methods described here can be efficiently implemented by using a recursive tree representation to calculate the required derivatives of the discrete Lagrangian and forcing function. The approach accommodates external forcing and holonomic constraints as described here, and is compatible with kinematic configuration variables [24], [32]. Additionally, this method could be extended to calculate higher derivatives if needed.

The authors have additionally used this framework to implement projection operator-based trajectory optimization [23] using variational integrators as the representation of the dynamics (these results will be presented in a future article).

## ACKNOWLEDGMENT

This material is based upon work supported by the National Science Foundation under award CNS 1329891 and IIS-0757378. Any opinions, findings, and conclusions or recommendations expressed in this material are those of the authors and do not necessarily reflect the views of the National Science Foundation.

## REFERENCES

- [1] E. Hairer, C. Lubich, and G. Wanner, *Geometric Numerical Integration*, ser. Springer Series in Computational Mathematics; 31. Springer-Verlag, 2004.
- [2] A. Lew, J. E. Marsden, M. Ortiz, and M. West, "Variational time integrators," *Int. J. Numer. Methods Engrg*, vol. 60, pp. 153–212, 2004.
- [3] —, "An overview of variational integrators," in *Finite Element Methods: 1970's and Beyond*, 2004, pp. 98–115.
- [4] A. Lew, "Variational time integrators in computational solid mechanics," *California Institute of Technology Thesis*, 2003.
- [5] B. Anderson and J. Moore, *Optimal Control: Linear Quadratic Methods*. Prentice Hall, Inc, 1990.
- [6] J. Zhong, J. Liu, and J. Shi, "Predictive control considering model uncertainty for variation reduction in multistage assembly processes," *IEEE Transactions on Automation Science and Engineering*, vol. 7, no. 4, pp. 724–735, 2010.
- [7] F. You, F. Wang, and S. Guan, "Game-theoretic design for robust  $h_\infty$  filtering and deconvolution with consideration of known input," *IEEE Transactions on Automation Science and Engineering*, vol. 8, no. 3, pp. 532–539, 2010.
- [8] E. R. Johnson and T. D. Murphey, "Scalable variational integrators for constrained mechanical systems in generalized coordinates," *IEEE Transactions on Robotics*, pp. 1249–1261, 2010.
- [9] A. Shiriaev, L. Freidovich, and S. Gusev, "Transverse linearization for controlled mechanical systems with several passive degrees of freedom," *IEEE Transactions on Automatic Control*, vol. 55, no. 4, pp. 893–906, 2010.
- [10] A. Laub, R. V. Patel, and P. M. V. Dooren, *The Control Handbook*, 2nd ed. CRC Press, 2010, vol. III: Control System Advanced Methods, ch. Numerical and Computational Issues in Linear Control and Systems Theory.
- [11] A. Hirani, "Linearization methods for variational integrators and Euler-Lagrange equations," *California Institute of Technology Thesis*, 2000.
- [12] S. Ober-Blöbaum, O. Junge, and J. Marsden, "Discrete mechanics and optimal control: An analysis," *ESAIM: Control, Optimisation and Calculus of Variations*, vol. 17, no. 2, pp. 322–352, 2011.
- [13] S. Leyendecker, S. Ober-Blöbaum, J. E. Marsden, and M. Ortiz, "Discrete mechanics and optimal control for constrained systems," *Optimal Control Applications and Methods*, vol. 31, no. 6, pp. 505–528, 2010.
- [14] J. Timmermann, S. Khattab, S. Ober-Blöbaum, and A. Trächtler, "Discrete mechanics and optimal control and its application to a double pendulum on a cart," in *Proc. of the 18th IFAC World Congress*, vol. 18, no. 1, Aug. 2011, pp. 10 199–10 206.
- [15] I. A. Şucan, M. Moll, and L. E. Kavraki, "The Open Motion Planning Library," *IEEE Robotics & Automation Magazine*, vol. 19, no. 4, pp. 72–82, 2012, <http://ompl.kavrakilab.org>.
- [16] R. D'Andrea, "Guest editorial: A revolution in the warehouse: A retrospective on kiva systems and the grand challenges ahead," *IEEE Transactions on Automation Science and Engineering*, vol. 9, no. 4, pp. 638–639, 2012.
- [17] E. Johnson and T. D. Murphey, "Linearizations for mechanical systems in generalized coordinates," in *American Controls Conference*, 2010, pp. 629–633.
- [18] M. Egerstedt, T. D. Murphey, and J. Ludwig, *Hybrid Systems: Computation and Control*, ser. Lecture Notes in Computer Science. Springer-Verlag, 2007, vol. 4416, ch. Motion Programs for Puppet Choreography and Control, pp. 190–202, eds. A. Bemporad, A. Bicchi, and G. C. Buttazzo.
- [19] L. Kharevych, W. Yang, Y. Tong, E. Kanso, J. E. Marsden, P. Schroder, and M. Desbrun, "Geometric, variational integrators for computer animation," *Eurographics/ACM SIGGRAPH Symposium on Computer Animation*, 2006.
- [20] M. West, "Variational integrators," *California Institute of Technology Thesis*, 2004.
- [21] J. E. Marsden and M. West, "Discrete mechanics and variational integrators," *Acta Numerica*, vol. 10, pp. 357–514, 2001.
- [22] R. Murray, Z. Li, and S. Sastry, *A Mathematical Introduction to Robotic Manipulation*. CRC Press, 1994.
- [23] J. Hauser and A. Saccon, "A barrier function method for the optimization of trajectory functionals with constraints," in *45th IEEE Conference on Decision and Control*, 2006, pp. 864 – 869.
- [24] E. Johnson, "Trajectory optimization and regulation for constrained discrete mechanical systems," Ph.D. dissertation, Northwestern University, 2012.
- [25] R. Featherstone, *Robot Dynamics Algorithms*. Kluwer Academic Publishers, 1987.
- [26] Y. Nakamura and K. Yamane, "Dynamics computation of structure-varying kinematic chains and its application to human figures," *IEEE Transactions on Robotics and Automation*, vol. 16, no. 2, 2000.
- [27] K. Yamane, *Simulating and Generating Motions of Human Figures*. Springer-Verlag, 2004.
- [28] E. Johnson, K. Morris, and T. D. Murphey, *Algorithmic Foundations of Robotics VIII*. Springer-Verlag, 2010, ch. A Variational Approach to Strand-Based Modeling of the Human Hand, pp. 151–166.
- [29] G. Rodriguez, A. Jain, and K. Kreutz-Delgado, "Spatial operator algebra for multibody system dynamics," *Journal of the Astronautical Sciences*, vol. 40, no. 1, pp. 27–50, 1992.
- [30] K. Anderson, "An order  $n$  formulation for the motion simulation of general multi-rigid-body constrained systems," *Computers & structures*, vol. 43, no. 3, pp. 565–579, 1992.
- [31] T. D. Murphey and E. Johnson, "Control aesthetics in software for automated marionettes," in *American Controls Conference*, 2011, pp. 3825–3830.

- [32] E. Johnson and T. Murphey, “Dynamic modeling and motion planning for marionettes: Rigid bodies articulated by massless strings,” in *International Conference on Robotics and Automation*, 2007, pp. 330–335.